

Application of an energy-based model for the optimal design of structural materials and topology

J. Du and J.E. Taylor

Abstract This paper describes an implementation of recent developments in modelling for the design of continuum structures into a general program for computational solution of such problems. In the basic model, the unrestricted material tensor appears as the design variable. The algorithm for this program is presented and the method of solution is described. The approach is applicable to predict both the optimal unrestricted material design and as well for design with a specified material. In either case, the distributions (fields) of all designable components of the material tensor are predicted. Results are given for 2D and 3D examples, in the form of continuously varying material properties and for various values of volume fraction. The associated zero-one or topology designs are obtained by application of an additional procedure to these results. Comparison against results from earlier approaches indicates that optimization of the material may lead to considerable improvement in structural performance.

Key words design optimization, continuum structures, optimum material properties, unrestricted material, optimal layout, optimal topology

1 Introduction

This paper has to do with the computational solution of problems in the optimal design of continuum structures, according to a formulation where the design variable is the unrestricted tensor field of material properties and where the argument of the cost constraint is

Received March 7, 2001

Revised manuscript received August 31, 2001

J. Du and J.E. Taylor

Aerospace Engineering, University of Michigan Ann Arbor,
MI 48109, USA

e-mail: jbd@engin.umich.edu, janos@engin.umich.edu

expressed in a general form. The formulation has the form of a maxmin variational problem covering both the mechanics of elastostatics and design optimization. The function and use of an algorithm for the computational treatment are described and a variety of solutions for design problems in 2D and 3D are presented. The behaviour of this system is explained both for determination of the optimal continuous-varying material properties, and for subsequent solution to predict a form of zero-one topology design. With these capabilities in mind, this basic model for structural optimization and its method of treatment for computation provides a possible alternative to the more commonly used approaches to the problem, namely those using homogenization-based modelling or some other form of simulation for interpretation of the continuum.

Because the subject matter of this paper relates to basic modelling in connection with a generalized form of structure, the material reported here is related at least implicitly to much of the earlier work on optimization of continuum structures. While it would be impractical to provide a survey of this material here, a few areas of precedent developments are cited and their relation to the present model is discussed. The reader is referred to the surveys by Rozvany (2001a,b) for a broader perspective on the subject. Michell truss design (see e.g. Michell 1904; Prager 1974; Prager and Rozvany 1977) is an early example among structural design problems where the design variables represent fields. Another example in kind is comprised of modelling for the design of grillages (Rozvany 1976) as the optimum design for flat structures that support loads in bending. Studies on the design of particular structural forms are reported by Olhoff *et al.* (1997) and Foldager (1999). On the more practical side, much work has been done to facilitate the modelling for design of finite composites. Pedersen (1993) provides a thorough treatment for design of structures composed of anisotropic materials. Liu *et al.* (2000) report on a two-level approach to the design of a composite wing structure. Mathematical modelling in continuum design is treated in depth by Cherkov (2000). A development in the direction of a more elemental formulation for

the optimization of continuum structures is described by (Bendsøe *et al.* 1994); there the unrestricted modulus tensor appears as the design variable field. The presentation of this paper relies on extensions of the latter approach, as indicated in the next section.

Following a brief presentation of the minmax formulation for the design problem of concern, an algorithm is described for the implementation of the problem into form for computational solution. The corresponding program, suitable for the prediction of optimal continuum structures in 2D and 3D, is exercised on a variety of examples. The material property fields predicted for these examples are pictured for all designable components of the elastic modulus tensor, and in some cases for several values of volume fraction. Results provide for a comparison of the relative efficiencies afforded by optimization at various levels, e.g. among the designs with fixed isotropic, variable isotropic, or unrestricted material properties, and between continuously varying versus zero-one material distributions.

2

Representation of the formulation for the local and global design

The basic model of (Bendsøe *et al.* 1994) for continuum design is extended (Taylor and Washabaugh 1995) into a form generalized with respect to statement of the resource or cost constraint. This generalized form is interpreted (Taylor 1998) in terms of an energy basis, which provides means for the expression in common of both unit energy and unit cost. As a final step toward the model implemented here, the energy formulation is restated (Taylor 2000) in a form where the design variable representing material properties fields is decomposed into global and local measures. With B and B_γ to represent, respectively, those measures, the formulation for analysis and minimum compliance design is stated as

$$\max_{B_\gamma; B} \left[\min_{c_\alpha; u_k} \left\{ \int_{\Omega} \sum_{\gamma=1}^M e_\gamma B_\gamma dV \right\} \right]$$

subject to

$$\left\{ \begin{array}{l} 0 < \underline{B}_\gamma \leq B_\gamma \leq \overline{B}_\gamma, \quad (\gamma = 1, A, M) \\ 0 < \underline{B} \leq B \leq \overline{B} \\ \sum_{\gamma=1}^M b_{L\gamma} B_\gamma - B \leq 0 \\ \int_{\Omega} bB dV - R \leq 0 \end{array} \right.$$

subject to

$$\left\{ \begin{array}{l} \underline{W} - \int_{\Omega} f_k u_k dV - \int_{\Gamma_t} t_k u_k \leq 0 \\ \frac{1}{2} (u_{i,j} + u_{j,i}) - \sum_{\alpha=1}^L c_\alpha \eta_{ij}^\alpha = 0 \end{array} \right., \quad (1)$$

where M is the number of components of the local material properties, and L represents the number of independent components of strain. In the 2D problem, for example, $M = 6$, $L = 3$. Again, elements B_γ of the energy basis identify the local material properties; η_{ij}^α symbolize a set of designated reference strains and c_α are coefficients such that $\sum_{\alpha=1}^L c_\alpha \eta_{ij}^\alpha$ evaluates the ij component of the strain tensor, \underline{W} is data representing a prescribed lower bound on compliance. When a set of reference strains is given, B_γ will have unique linear relationship with the elasticity modulus tensor \mathbf{E}_{ijkl} (Taylor 1998). Argument $\int_{\Omega} \sum_{\gamma=1}^M e_\gamma B_\gamma dV$ in (1) evaluates total strain energy, and so e_γ may be interpreted as the strain energy density per unit B_γ . Design variable B represents the distribution within Ω of material resource, as a measure of global material distribution; $b_{L\gamma}$ and b represent correspondingly the unit cost of local properties and global material distribution. The inner part of (1) is in effect an isoperimetric form of the minimum potential energy formulation for elastostatics. It reflects minimization of the strain energy within an isoperimetric constraint on the measure of compliance. Here the strain energy is represented in terms of the energy basis B_γ ; u_k represents the displacement field, f_k and t_k are correspondingly the body forces in structure occupying region and traction on the traction boundary Γ_T .

Considering the “max” of (1) governing design, B_γ and B appear as variationally independent. This feature is used to advantage in the computational implementation described below, namely to provide for the prediction separately of global distribution of resource and local material properties.

From problem (1), the design for local properties may be stated as

$$\max_{B_\gamma} \left\{ \int_{\Omega} \sum_{\gamma=1}^M e_\gamma B_\gamma dV \right\}$$

subject to

$$\left\{ \begin{array}{l} 0 < \underline{B}_\gamma \leq B_\gamma \leq \overline{B}_\gamma, \quad (\gamma = 1, A, M) \\ \sum_{\gamma=1}^M b_{L\gamma} B_\gamma - B \leq 0 \end{array} \right\} \quad (\text{for } x \in \Omega). \quad (2)$$

Here it is implicit that the global material distribution $B(x)$ is specified and remains fixed. Notice that the constraints in problem (2) are point-wise constraints, so the integral in the objective function could be put out-

side of the symbol of “max”. With this transformation, the point-wise design of local properties is governed by

$$\max_{B_\gamma} \left\{ \sum_{\gamma=1}^M e_\gamma B_\gamma dV \right\}$$

subject to

$$\left\{ \begin{array}{l} 0 < \underline{B}_\gamma \leq B_\gamma \leq \overline{B}_\gamma, \quad (\gamma = 1, A, M) \\ \sum_{\gamma=1}^M b_{L\gamma} B_\gamma - B \leq 0 \end{array} \right\}$$

$$(\text{for each } x \in \Omega). \quad (3)$$

Accordingly, it provides for the computational determination of the optimal local properties, for given distribution B .

For convenience in the description to follow, consider relative to a given set of local properties B_γ the set of similar materials, say β_γ , defined by

$$\beta_\gamma = r B_\gamma. \quad (4)$$

Identify by (β_γ^*, r^*) the particular similar material field that satisfies the constraint

$$\sum_{\gamma=1}^M b_{L\gamma} \beta_\gamma^* = B. \quad (5)$$

Then the associated scale factor r^* is given by

$$r^* = \frac{B}{\sum_{\gamma=1}^M b_{L\gamma} \beta_\gamma}. \quad (6)$$

This scaling is used in the algorithm presented below, for stepwise adjustment to meet the constraint. Note that all quantities are identified with fields $B_\gamma(x)$ and $B(x)$, and that the scaling $r^*(x)$ is generally not uniform.

Next we consider the other part of the two-part cycle for computation, namely the prediction of global distribution of resource for a specified fixed material. For a fixed set of local properties B_γ , the coefficient e , a measure of average unit energy, is defined by

$$e := \frac{\sum_{\gamma=1}^M e_\gamma B_\gamma}{\sum_{\gamma=1}^M b_{L\gamma} \beta_\gamma}. \quad (7)$$

Taking into account the constraint in (3) relating B and B_γ , the part of (1) governing design of B may now be stated as

$$\max_B \left\{ \int_{\Omega} e B dV \right\}$$

subject to

$$\left\{ \begin{array}{l} 0 < \underline{B} \leq B \leq \overline{B} \\ \int_{\Omega} b B dV - R \leq 0 \end{array} \right\}. \quad (8)$$

Here coefficient e may be interpreted as the strain energy density per unit global material distribution measure B . Equation (8) provides for the computational determination of the optimal global material distribution, for specified local properties B_γ .

3 The algorithm

The algorithm is constructed in a way to produce sequential updating of B and B_γ , according to (8) and (3), respectively. Iteration is done between the two design parts to acquire the final results having both optimal global material distribution and optimal local properties. During the update step for design of global distribution B , the local properties are held fixed, and vice versa. The algorithm for the simultaneous design of global material distribution and local properties is described below (where the super index “ g ” represents the count of outer cycle of design).

- Step 1. Introduce the initial values of local properties $B_\gamma^{(0)}$ and global material distribution measure $B^{(0)}$.
- Step 2. For the first part of the g -th cycle, solve for optimal global material distribution for local properties $B_\gamma^{(g)}$, and get new global material distribution measure $B^{(g+1)}$.
- Step 3. Still in the g -th cycle, solve for optimal local properties in each point (or element, for discrete computation) for global material distribution $B^{(g+1)}$, to predict new local properties $B^{(g+1)}_\gamma$.
- Step 4. To complete the g -th cycle, compute the similar local material properties $B_\gamma^{*(g+1)}$ which satisfy the constraints $\sum_{\gamma=1}^M b_{L\gamma} \beta_\gamma^{*(g+1)} = B^{(g+1)}$.
- Step 5. Convergence checking: if converged, then stop; if not converged, then go back to Step 2 and begin a new cycle.

In the computation, the order of Steps 2 and 3 may be exchanged. For the global design in Step 2 and local design in Step 3, an inner iteration could be introduced, at the same time, the mechanics analysis is necessary in each sub-design in order to get the modified e_γ and e , i.e. the strain energy density per unit component of local properties and per unit global material resource distribution measure. Prediction of global design and local design respectively are described by the flow-charts in Figs. 1 and 2 (where the lower index “ k ” represents the count of the inner cycle of design).

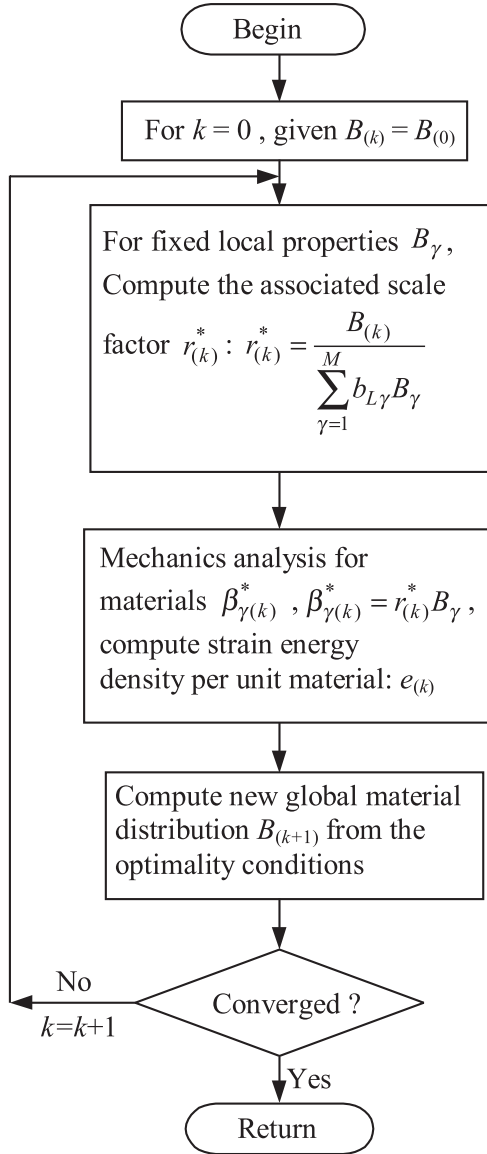


Fig. 1 Flow-chart 1. Design of global material distribution

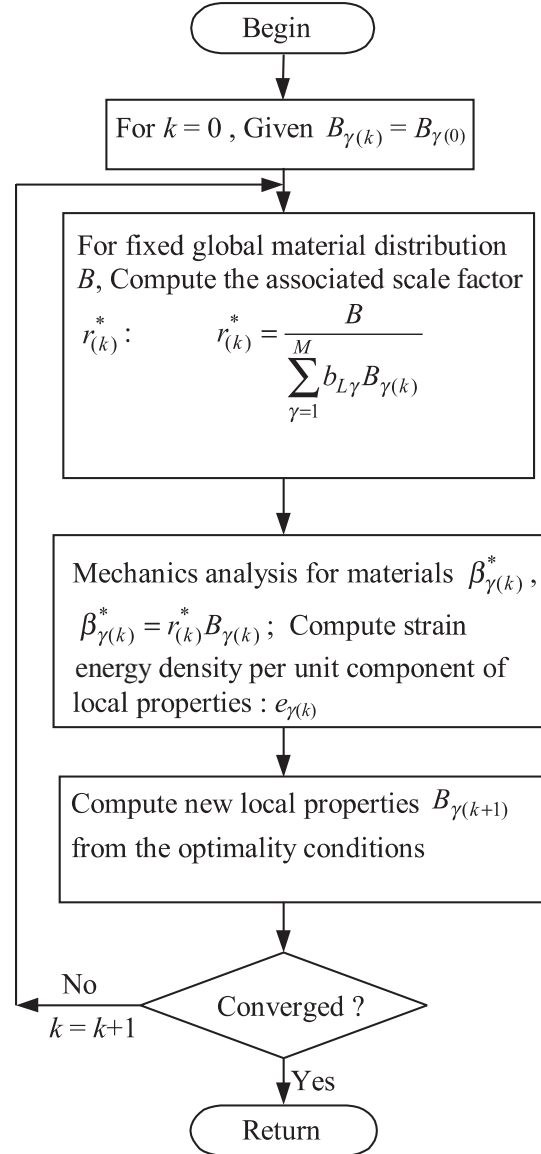


Fig. 2 Flow-chart 2. Design of local properties

3.1

A scheme to update local material properties and material resource distribution based on the optimality conditions

The optimality conditions are used in the update schemes for the computation of the global material distribution and local properties. The update of global design B is obtained using

$$B_{(k+1)} = \frac{e_{(k)}}{b\tilde{e}_{(k)}} B_{(k)}, \quad (9)$$

where $\tilde{e}_{(k)}$ is determined by the constraint of global material resource; initially, $\tilde{e}_{(k)}$ may be defined as

$$\tilde{e}_{(k)} = \frac{\int_{\Omega} e_{(k)} B_{(k)} dV}{R} = \frac{U_{(k)}}{R}. \quad (10)$$

Here, $\tilde{e}_{(k)}$ represents the average strain energy per unit resource. Similarly, the update of local properties is governed by

$$B_{\gamma(k+1)} = \frac{e_{\gamma(k)}}{b_{L\gamma}\tilde{e}_{\gamma(k)}} B_{\gamma(k)}. \quad (11)$$

3.2

Scaling computation of material measurement and properties

A scaling procedure will be introduced into the update model of material measure and properties in order to satisfy the resource constraints. Taking the computation of global material measure B as example, the initial value of scaling factor α_0 could be solved by the following equation:

$$\alpha_0 \int_{\Omega} bB \, dV = R. \quad (12)$$

Then a sub-cycle to compute the final scaling factor α is needed to make both global and local resource constraints be satisfied (where the lower index “ s ” represents the count of the scaling cycle) (see Fig. 3 below).

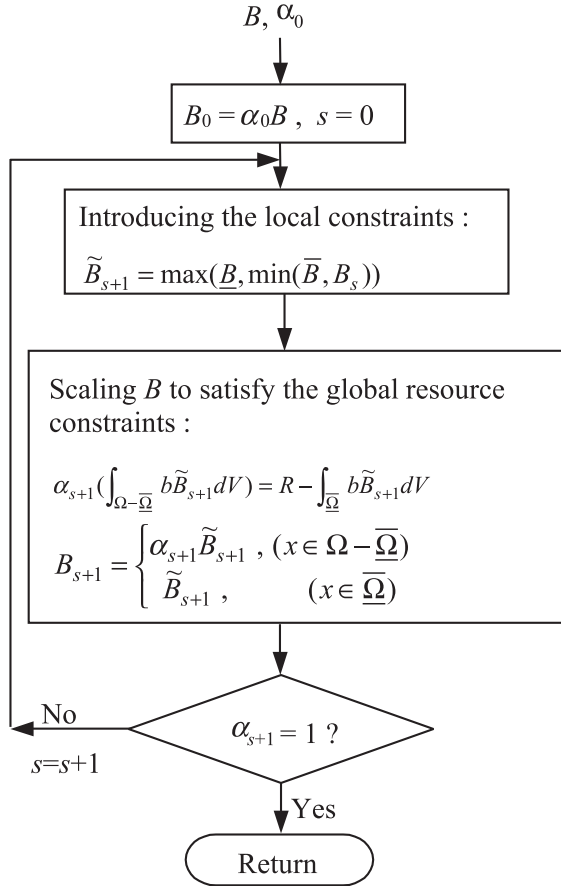


Fig. 3 Flow-chart 3. Scaling computation of global resource measure

In flow-chart 3, $\underline{\Omega}$ represents the area where $B_{s+1} = \underline{B}$ or $\tilde{B}_{s+1} = \underline{B}$.

3.3

Simplification of the optimal design for isotropic local properties

As indicated in the introduction, the general approach to predict the optimal continuum may be applied as well in cases where local properties are restricted. As an example, (see Figs. 16–19), when the available material for the design is confined to be isotropic, the number of independent components of material is reduced to 2. If we choose the same reference strains as were used in the paper (Taylor 1998), the additional constraints among design variables (for 2D problem, $\gamma = 1, \dots, 6$) that would result in isotropic material are written as

$$\begin{aligned} B_1 + B_2 - 2B_5 &= 0, & B_2 + B_3 - 2B_6 &= 0, \\ B_1 - B_3 &= 0, & 2B_2 - 3B_1 - B_3 + 2B_4 &= 0. \end{aligned} \quad (13)$$

There are two ways to activate these constraints during the computational procedure. One way is to modify the formula of resource constraints in the design of local properties as

$$\begin{aligned} \sum_{\gamma=1}^M b_{L\gamma} B_\gamma + b_{LI} |B_1 + B_2 - 2B_5| + b_{LII} |B_2 + B_3 - 2B_6| + \\ b_{LIII} |B_1 - B_3| + b_{LIV} |2B_2 - 3B_1 - B_3 + 2B_4| \leq B, \end{aligned} \quad (14)$$

where the additional coefficients b_{LI} , b_{LII} , b_{LIII} , b_{LIV} take on value large relative to the original cost coefficients. Another way is to directly eliminate the redundant design variables using (13). Then only two independent design variables, say: B_2 and B_4 remain and the simplified design problem of local properties is restated as (for 2D problem)

$$\begin{aligned} \max_{B_\gamma} \left\{ \sum_{\gamma=2,4} \tilde{e}_\gamma B_\gamma \, dV \right\} \\ \text{subject to} \\ \left\{ \begin{aligned} 0 < \underline{B}_\gamma \leq B_\gamma \leq \overline{B}_\gamma, \quad (\gamma = 2, 4) \\ \sum_{\gamma=2,4} \tilde{b}_{L\gamma} B_\gamma - B \leq 0 \end{aligned} \right\} \\ \text{(for each } x \in \Omega), \end{aligned} \quad (15)$$

where

$$\begin{aligned} \tilde{b}_{L2} &= b_{L2} + \frac{1}{2}(b_{L1} + b_{L3}) + \frac{3}{4}(b_{L5} + b_{L6}), \\ \tilde{b}_{L4} &= b_{L4} + \frac{1}{2}(b_{L1} + b_{L3}) + \frac{1}{4}(b_{L5} + b_{L6}), \end{aligned} \quad (16)$$

$$\begin{aligned} \tilde{e}_2 &= e_2 + \frac{1}{2}(e_1 + e_3) + \frac{3}{4}(e_5 + e_6), \\ \tilde{e}_4 &= e_4 + \frac{1}{2}(e_1 + b_3) + \frac{1}{4}(e_5 + e_6). \end{aligned} \quad (17)$$

3.4

Implementation for the design of structural topology

When the relative unit cost b is uniformly distributed in the global design area, the solution of problem (1) is the optimal global material distribution B with optimal local properties B_γ . The distribution of B in the global design area depicts the function as “shades of gray”. However, where it would be of interest, a method is available to generate structural topology, i.e. the so called “zero-one” or “black & white” design. By adjusting the value of relative unit cost b according to the value of B , one can

generate the “black & white” design from the “shades of gray” design. The basic idea is similar to the method of papers (Guedes and Taylor 1997; Rodrigues *et al.* 1999). Firstly, defining a set of cutoff value of global material measure B_k^c ,

$$B_k^c = B_{k,\min} + \eta_k \frac{k}{N} (\bar{B} - B_{k,\min}), \quad (k = 1, 2, \dots, N), \quad (18)$$

where $B_{k,\min} = \max(\min(B_k), \underline{B})$, η_k is a factor to control the step size of the cutoff value of the k -th step ($0 < \eta_k \leq 1$). For the k -th step, the unit cost of global material distribution b will be adjusted according to the value of B

$$b_k = \begin{cases} 1 & (\text{for } B_k \geq B_k^c) \\ \bar{b}_k & (\text{for } B_k < B_k^c) \end{cases} \quad (k = 1, 2, \dots, N), \quad (19)$$

where \bar{b}_k increased gradually with k increased, $\bar{b}_k > 1$ and $\bar{b}_N \gg 1$. The update model of global material distribution will be modified as

$$B_{k+1} = \frac{e_k}{b_k^\xi \bar{e}_k} B_k \quad (\xi > 1), \quad (20)$$

where factor ξ is introduced to assure the area Ω^- with material measure B under the cutoff value is real “white area”, i.e. $\int_{\Omega^-} \bar{b}_{N-1} B_N dV \ll R$.

Another way to implement the “black & white” design from the “shades of gray” design is to introduce a penalty factor p into the update model of global material distribution. When B_{k+1} is acquired from the original update model (9), which represents the state of currently global material distribution, then the penalty factor p is applied to make the gray part under the cutoff value approach “white”,

$$\tilde{B}_{k+1} = \left(\frac{B_{k+1}}{B_k^c} \right)^p B_k^c, \quad (21)$$

where

$$p = \begin{cases} 1 & (\text{for } B_{k+1} \geq B_k^c) \\ \bar{p} & (\text{for } B_{k+1} < B_k^c) \end{cases} \quad (k = 1, 2, \dots, N), \quad (22)$$

where $\bar{p} > 1$, and it is usually a better way to set the value of \bar{p} gradually increase with k increases. A proper choice of the value of \bar{p} is between 2 and 4.

4

On computation and example solutions

As might be expected with a computational effort of the present kind, issues arise in connection with conditioning for stability, convergence, and efficiency. Detailed consideration of such concern is outside the scope of this paper.

However, certain aspects of concern in the computation are treated here in brief.

One issue is about the checkerboard phenomenon, which exists in the solutions of this paper since the displacement based numerical implementation is used to compute the strain energy. To eliminate the checkerboard, the mesh-independent filter (Sigmund 2000) is introduced in our program, which will not increase the cpu-time remarkably. Another issue is about the definition of the set of admissible materials. For a real structure, the strain energy should always be positive. But in the model of this paper, the constraints to the material components are not sufficient to guarantee the strain energy positive. An exception is, in 2D design, when the materials are confined to be isotropic, the local constraints to B_γ will be able to keep the strain energy always positive. For the design for arbitrary material, a simple and effective technology is employed in the computational procedure to keep the strain energy positive, which avoids the trouble that introducing some nonlinear constraints of material components to keep the materials positive definition. The idea is, when we start from a point in the positive definition material space, and get the updated material point from the optimality conditions, we execute a linear search to find a new point between the two points. This new point must satisfy the following conditions: located in the positive definition material space and be closest to the updated material point. An extreme case is, the updated material point itself is positive definition, then this point is the new point and will be used as the starting point of the next iteration. This procedure can be expressed by a linear design problem with single design variable for each element, and it is very easy to be solved. Numerical examples show it works very well.

In the aspect of the representation of material components, since the value of each component E_{ijkl} usually varies with different coordinates, sometimes people are more concerned about the value of those components in special coordinates in order to identify some characteristic of the material. For example, the coordinate projected onto direction identified with principal stress. The transformation of material matrix between coordinates $x-y$ and $x'-y'$ may be stated as

$$\mathbf{D}' = \mathbf{T}_\sigma \mathbf{D} \mathbf{T}_\varepsilon^{-1} = \mathbf{T}_\sigma \mathbf{D} \mathbf{T}_\sigma^T, \quad (23)$$

$$\boldsymbol{\sigma}' = \mathbf{T}_\sigma \boldsymbol{\sigma}, \quad (24)$$

$$\boldsymbol{\varepsilon}' = \mathbf{T}_\varepsilon \boldsymbol{\varepsilon}, \quad (25)$$

where $\boldsymbol{\sigma}'$, $\boldsymbol{\varepsilon}'$, \mathbf{D}' are stress, strain vectors and material matrix in coordinate $x'-y'$, $\boldsymbol{\sigma}$, $\boldsymbol{\varepsilon}$, \mathbf{D} are stress, strain vectors and material matrix in coordinate $x-y$; \mathbf{T}_σ , \mathbf{T}_ε are the transformation matrix of stress and strain vectors. With this transformation applied in each point of structure, the figure of material components in the point-wise varied principal coordinates will be acquired.

4.1

Example 1. Optimization of materials and topology for unrestricted local properties

This example will show the complete results of the simultaneous design of local properties and global material distribution, from which we could see the general characteristic of the optimal local properties, global material distribution and structural topology under single load design.

Results presented here indicate designs for a structure to carry a uniform load over a region of specified aspect ratio. The design space, support surfaces, and loading are shown in Fig. 4. The thickness of the sheet $t = 0.01$ (all of the parameters in the computation use interna-

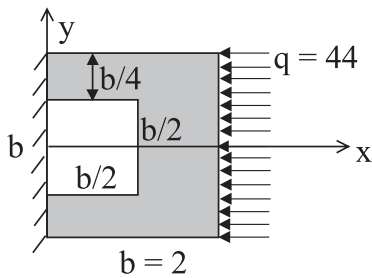
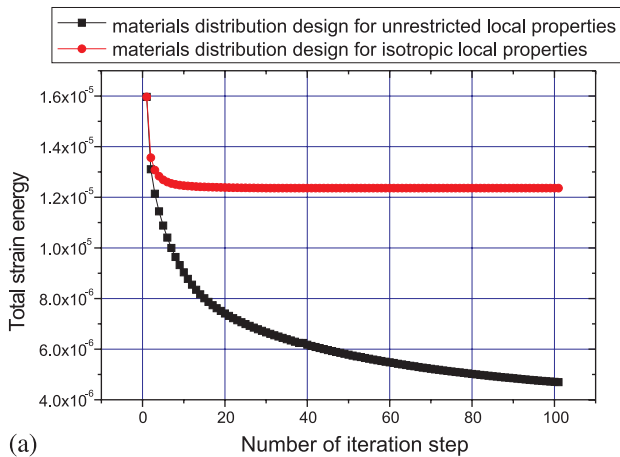


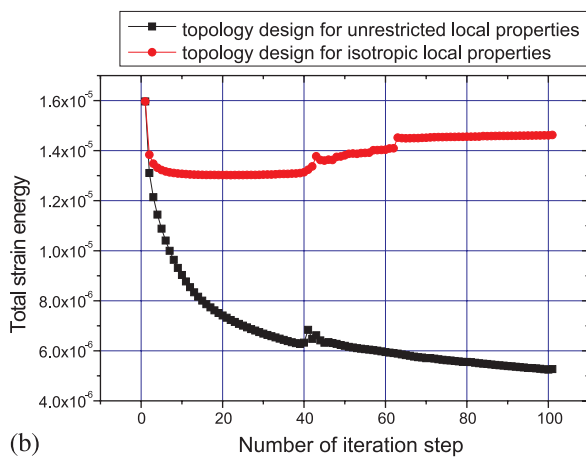
Fig. 4 Sheet with square hole and uniform load on the right boundary

tional unit). From the symmetry, only the upper half of the structure is considered in design, with proper constraints applied on the symmetric plane. The initially used material is isotropic material and distributed uniformly over global design area. The initial value of local properties are: $E = 10^{11}$, $\nu = 0.3$. For the given reference strains (Taylor 1998), the corresponding value of the basis of strain energy are: $B_1 = 5.495 \times 10^{10}$, $B_2 = 3.846 \times 10^{10}$, $B_3 = 5.495 \times 10^{10}$, $B_4 = 7.143 \times 10^{10}$, $B_5 = 4.670 \times 10^{10}$, $B_6 = 4.670 \times 10^{10}$. The upper bound of the measurement of global material distribution, $\bar{B} = 1.5 \times 10^{12}$, in topology design, this value will make the available resource equals 44% of the volume of the design domain. The lower bound of the measurement of global material distribution, $\underline{B} = \bar{B} \times 10^{-9}$. The unit cost of local material properties: $b_\gamma = 1$ ($\gamma = 1, 2, \dots, 6$), the initial value of unit cost of the measurement of global material distribution: $b = 1$, and uniformly distributed over design area. The half of the design area is divided by 47×23 mesh.

In the first case (Figs. 5 to 12), the topology of a single-bay arch and its superstructure is predicted, both for unrestricted design space and where the structure is to span a specified hole. Figure 5 shows the variation of total strain energy with iteration, we could see the strain energy history curve of the design for isotropic local properties converged very quickly. Figure 5a shows the results of the design of global material distribution, the

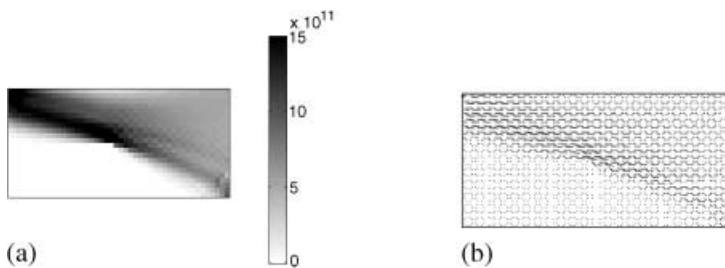


(a)



(b)

Fig. 5 Variation of total strain energy with iteration number. (a) Materials distribution design (b) topology design



(a)

(b)

Fig. 6 Results of materials distribution design for unrestricted local properties (only one half of the original structure from the symmetry of the structure shown). (a) Optimal global materials distribution, (b) direction of the first principal stress

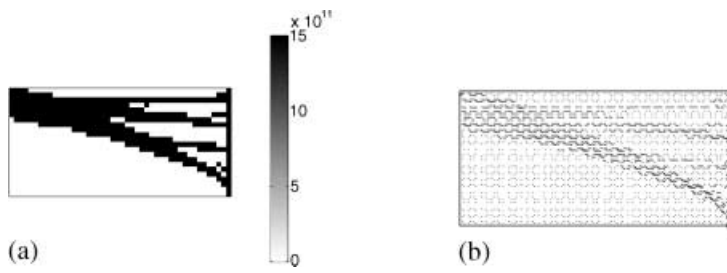


Fig. 7 Results of topology design for unrestricted local properties. (a) Optimal topology, (b) direction of the first principal stress

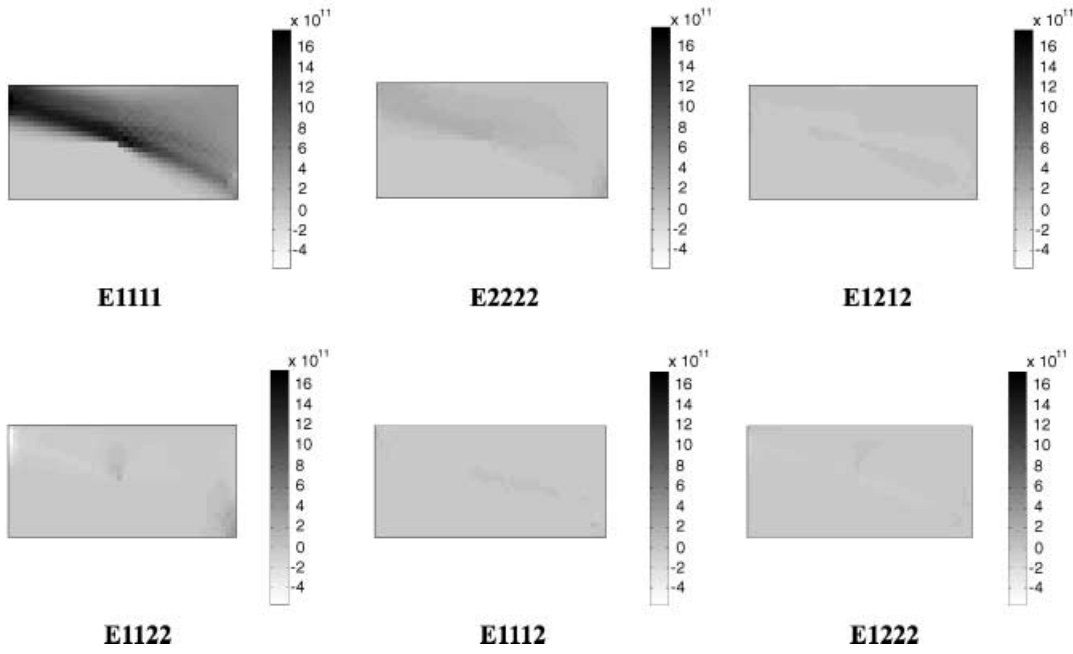


Fig. 8 Optimal local properties projected onto directions identified with principal stresses (for material distribution design)

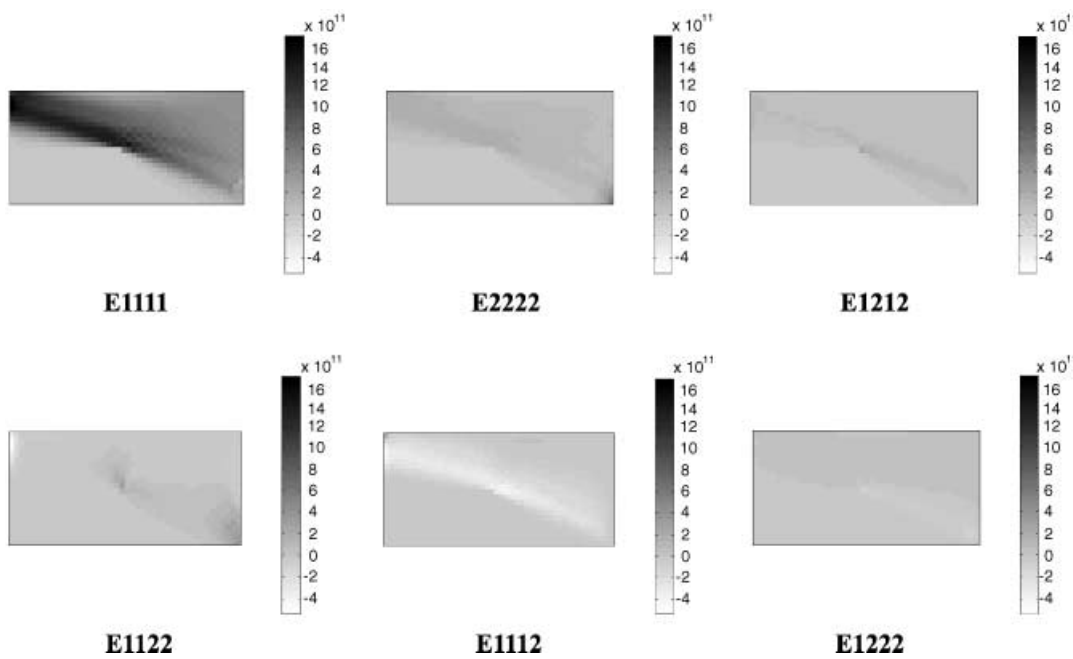


Fig. 9 Optimal local properties in the original x - y coordinates (for material distribution design)

two curves represent correspondingly the design for unrestricted local properties and isotropic local properties. The final design results for isotropic materials is 25% better than the initial results, and the final design results for unrestricted materials is 70% better than the initial results. The similar results appeared in topology design. This evinces the design for unrestricted local properties will greatly improve the compliance of the system.

Figures 6 and 7 show the results of optimal global material distribution and optimal topology, and the corresponding

direction of maximum principal stress. In Fig. 8, the optimal local properties projected onto directions identified with principal stresses in material distribution design are shown. For comparison, the optimal local properties in the original x - y coordinates are shown in Fig. 9. The corresponding results of optimal local properties in topology design are shown in Figs. 10 and 11. Please note the region of negative value for components E_{1112} and E_{1222} in the fixed original coordinate (Figs. 9, 11). From Figs. 8 and 10, for the optimal local properties, the

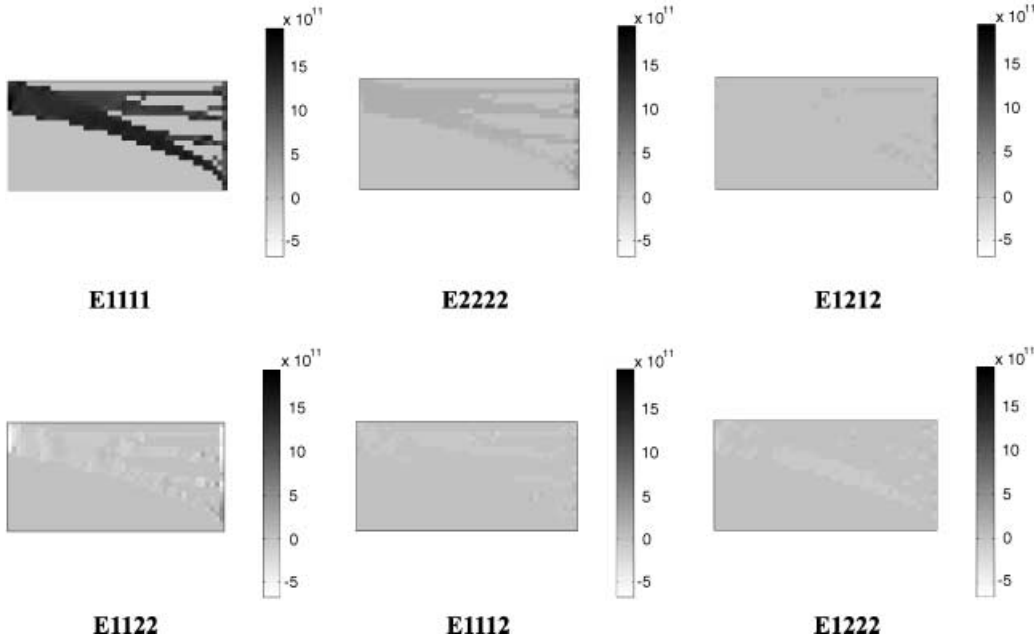


Fig. 10 Optimal local properties projected onto directions identified with principal stresses (for topology design)

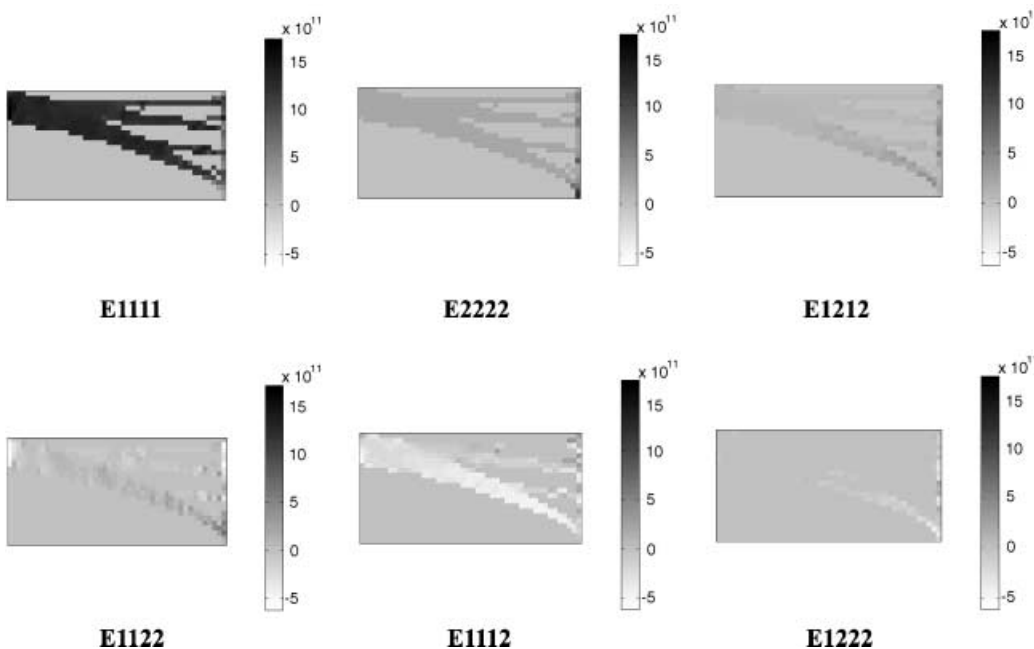


Fig. 11 Optimal local properties in the original x - y coordinates (for topology design)

components of E_{1112} , E_{1222} and E_{1212} are very weak in the point-wised principal coordinates, which are apparently different from the results in the original coordinates. Meanwhile, the E_{1111} component is much larger than E_{2222} and E_{1212} components in the principal coordinates. It denotes that, in the principal coordinates, the optimal distribution of local properties approaches to make the materials concentrate to the components which mostly sustain the tension and pressure, i.e. E_{1111} , E_{2222} and E_{1122} components. For comparison, the optimal distribu-

tion of strain energy basis (B_γ) in topology design are shown in Fig. 12. For a group of fixed reference strains, B_γ is invariant.

As an interesting comparison to the design for unrestricted local properties, Fig. 13 shows the results of global material distribution and topology in design for materials restricted in isotropic scope, where the numbers of independent material components are 2. In Fig. 14, the distribution of two important elasticity constants for isotropic materials, Young's modulus E and Pois-

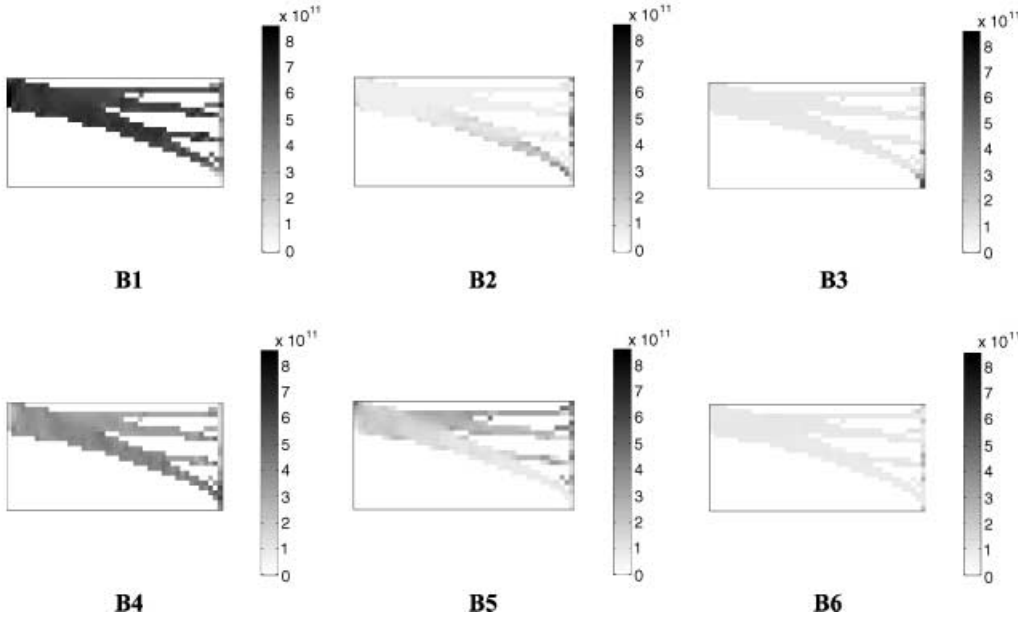


Fig. 12 Optimal distribution of strain energy basis for topology design

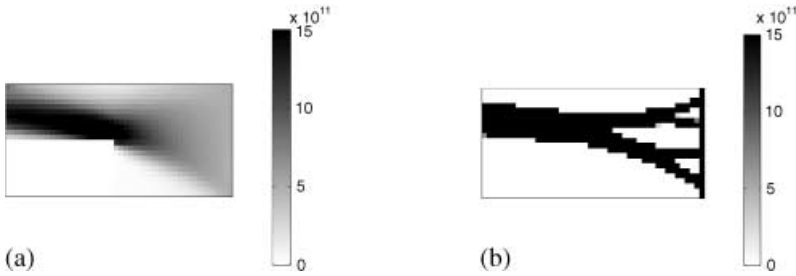


Fig. 13 Results of design for variable isotropic materials. (a) Optimal global material distribution, (b) optimal topology

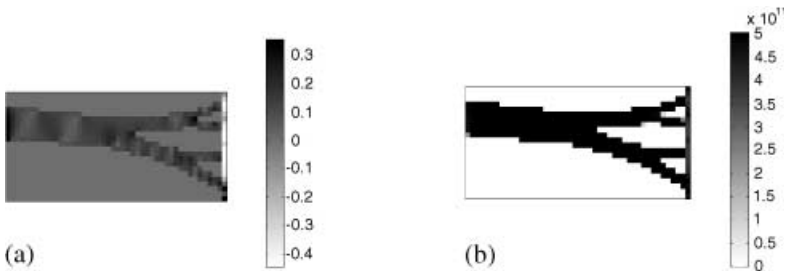


Fig. 14 Optimal isotropic local properties for topology design. (a) Optimal Poisson's ratio, (b) optimal Young's modulus E

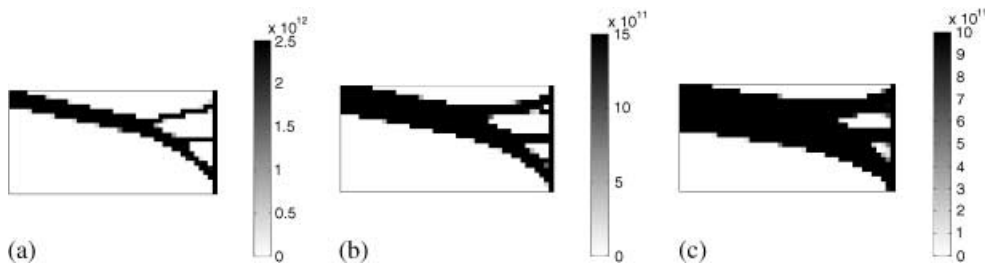


Fig. 15 Optimal topology for three values of volume fraction (fixed isotropic materials). Volume fractions: (a) 20%, (b) middle 33%, (c) 50%

son's ratio ν , are given. In order to identify the distribution of Poisson's ratio clearly in optimal topology, the Poisson's ratio of the materials in "white" area is set to zero in Fig. 14a. It's very interesting to see that, in some area of the optimal topology, the Poisson's ratio is negative. For the global structure, the value of Poisson's ratio varies approximately from -0.4 to 0.3 . According to the positive definition of strain energy, we know the value of Poisson's ratio in theory can be varied from -1 to 0.5 . But in engineering, the materials with negative Poisson's ratio are very unusual. This example shows an application of such kind of materials, i.e. in material design problems, if the materials

with negative Poisson's ratio are filled into some special area of the structure, the global structure may be more stiffening.

Results for the design of the above structure without a specified hole are given for several values of volume fraction. The topology of their superstructures are also predicted (Fig. 15), all for fixed isotropic material. The following cases (Figs. 16a,b and c) show the multiple-bay results for different ratios of length and height of structures, which are produced for longer bridge spans. From which we may see the interesting topology evolution of the middle arch with the increase of the length of the bridge.

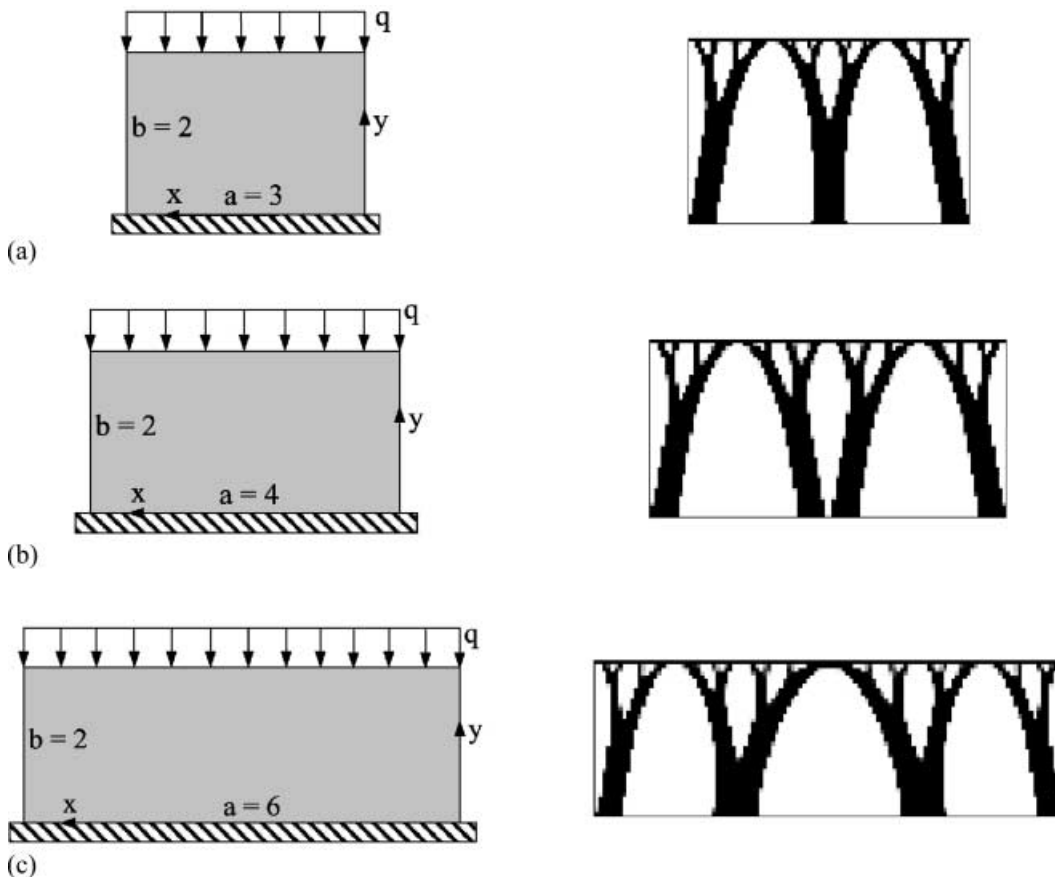


Fig. 16 Optimal topology for multiple-bay results with different ratios of length and height (all for 33% volume fraction, fixed isotropic materials). (a) Length: height = $1.5 : 1$, (b) length: height = $2 : 1$, (c) length: height = $3 : 1$

4.2

Example 2. Multiple loads design of rectangular sheet with prescribed hole

This is an example of multiple load design for simultaneous optimization of local properties and global material distribution.

Figure 17 shows a rectangular sheet with a prescribed square hole. Three kinds of symmetric load cases are considered. Case 1: the horizontal loads. Case 2: the vertical loads. Case 3: the horizontal and vertical loads simultaneously applied. Since the loads are symmetric, the structure will be able to keep equilibrium without additional boundary constraints.

The thickness of the sheet $t = 0.01$. From the symmetry, only one quarter of the structure is considered in design, with proper constraints applied on the horizontally and vertically symmetry plane. The material used for the initial design is isotropic and distributed uniformly over the global design area. The material parameters are the same as example 1. The upper bound of the measurement of global material distribution, $\bar{B} = 2.0 \times 10^{12}$. In topology design, this value will make the available resources occupy 28% of the volume of the design domain. The lower bound of the measurement of global material distribution, $\underline{B} = \bar{B} \times 10^{-9}$. The unit cost of local ma-

terial properties: $b_\gamma = 1$, and uniformly distributed over design area. One quarter of the design area is divided by 47×23 mesh.

The design objective of multiple loads cases above may be written as a linear combination of strain energies of all loads cases:

$$\bar{U} = \alpha_1 \left(\int_{\Omega} \sum_{\gamma=1}^M e_\gamma^1 B_\gamma dV \right) + \alpha_2 \left(\int_{\Omega} \sum_{\gamma=1}^M e_\gamma^2 B_\gamma dV \right) + \alpha_3 \left(\int_{\Omega} \sum_{\gamma=1}^M e_\gamma^3 B_\gamma dV \right). \tag{26}$$

Where e_γ^1 , e_γ^2 and e_γ^3 are corresponding to loads case 1, case 2, and case 3 in which the loads case 1 and 2 are applied simultaneously; α_1 , α_2 and α_3 are weights of strain energy, which may be varied from 0 to 1. The initial material used is isotropic material ($E = 10^{11}$, $\nu = 0.3$), distributed uniformly over the global design domain.

Considering α case 1: $\alpha_1 = \alpha_2 = \frac{1}{2}$, $\alpha_3 = 0$ (filter introduced).

In this example, 31 iteration steps are executed. The total computational time is about 15 minutes.

Figure 18a shows the results of topology design for α case 1, the initial weighted total strain energy of system is

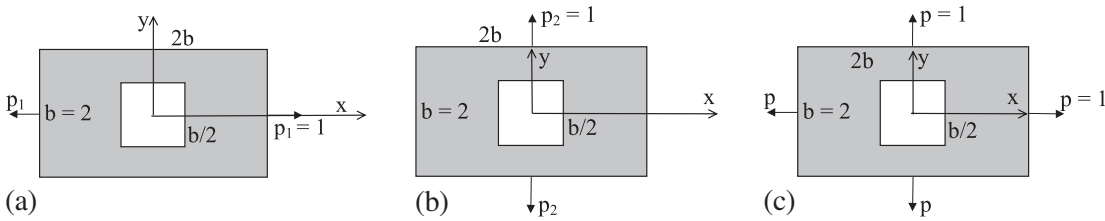


Fig. 17 Multiple loads design. (a) Single load case 1 (horizontal loads), (b) single load case 2 (vertical loads), (c) single load case 3 (horizontal and vertical loads)

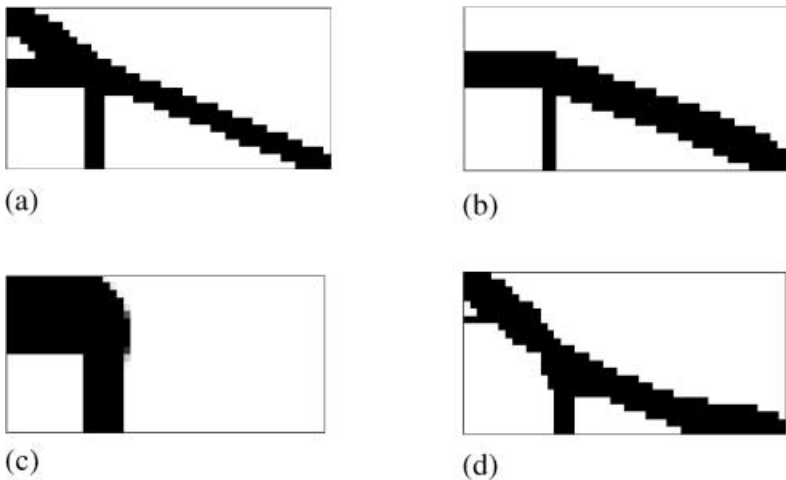


Fig. 18 Optimal topology for different load cases (U is the total strain energy; only one quarter of the original structure from the symmetry shown). (a) Multiple loads design ($\bar{U} = 0.520 \times 10^{-9}$), (b) single load design (case 1) ($U = 0.387 \times 10^{-9}$), (c) single load design (case 2) ($U = 0.430 \times 10^{-9}$), (d) single load design (case 3) ($U = 0.624 \times 10^{-9}$)

$\bar{U} = 2.456 \times 10^{-9}$, the final weighted total strain energy of system is $\bar{U} = 0.520 \times 10^{-9}$. The iteration converged after about 15 steps and the final result is 79% better than the initial result from the total strain energy.

4.3 Comparison of the results between multiple load design and single load design

Figures 18a–d compare the optimal topology in multiple load design and three kinds of single load design; \bar{U}

and U represent respectively the total strain energy of multiple load design and single load design. In multiple load design, both of the beams along horizontal and vertical direction are strong, which will provide enough stiffness for both load case 1 and case 2. But in the single load design (cases 1, 2 and 3), apparently the structural layout can not provide enough stiffness for all of the three load cases. In addition, for the multiple load design, the proportion of the weight coefficient α can be adjusted to emphasize one of the single load cases.

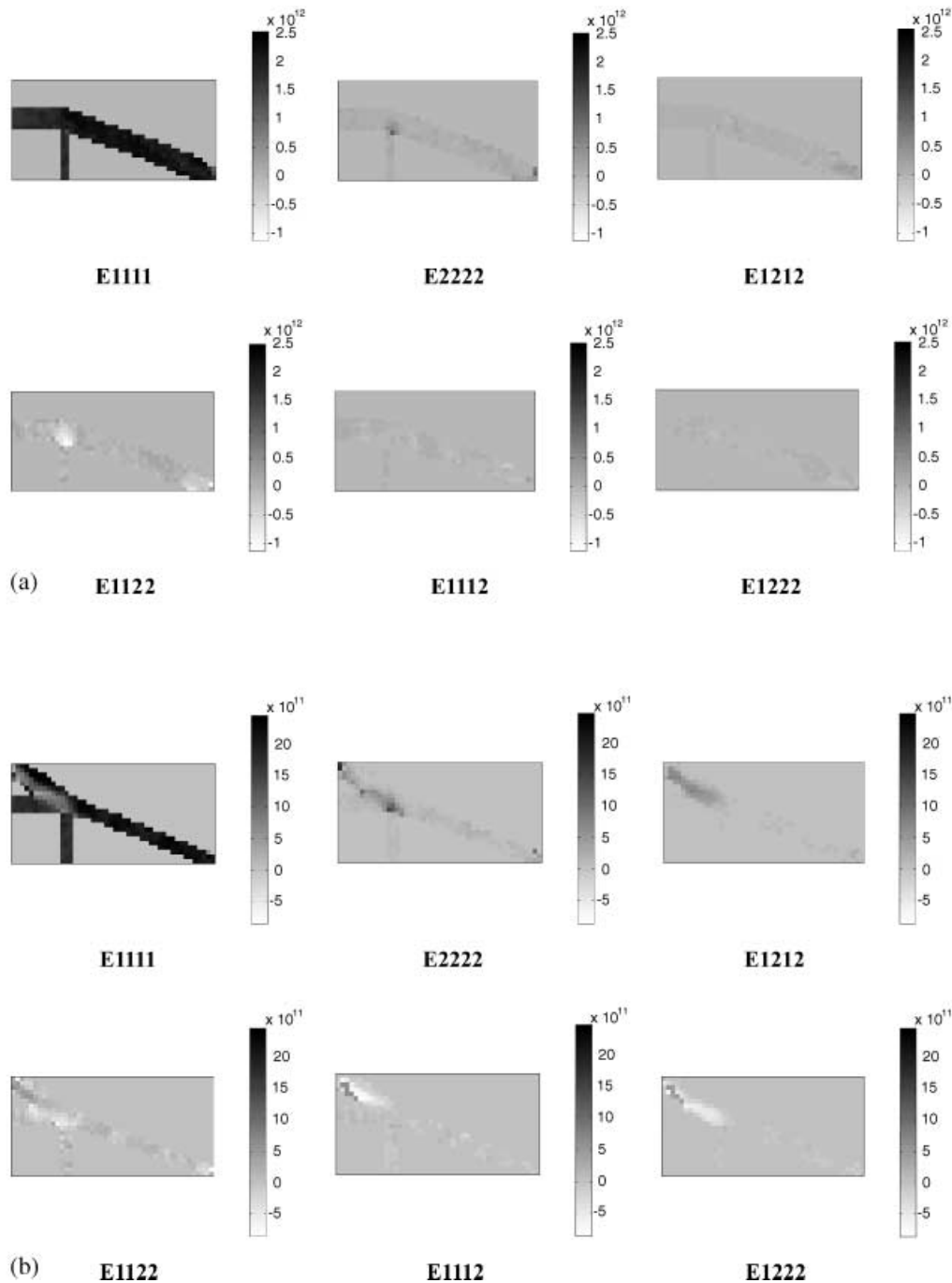


Fig. 19 Optimal local properties projected onto directions identified with principal stresses of load case 1. Single load design (case 1)

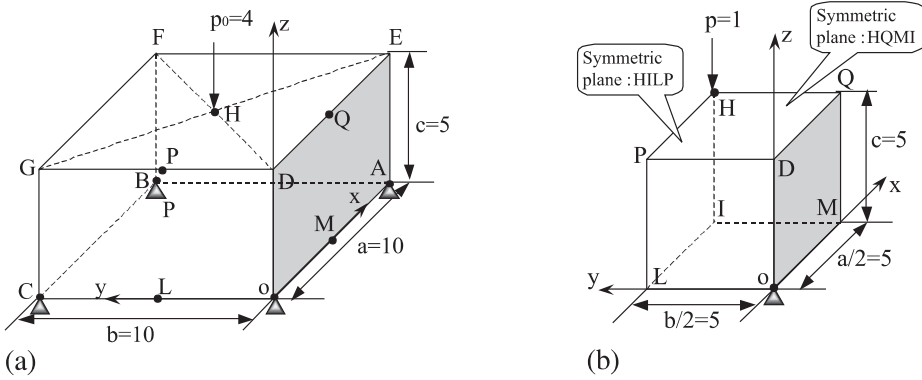


Fig. 20 3D thick plate with simple supports on its four corners and bending load. (a) Design domain and load conditions, (b) one quarter of original design domain (used for optimal design)

Figures 19 and 20 compare the optimal local properties in single load design case 1 and multiple load design. From Fig. 19 we could see, for single load design, the optimal local properties are basically orthotropic (E_{1112} and E_{1222} are very weak), meanwhile, E_{1212} is also very weak, so we could draw the same conclusion as example 1. But for multiple load design, the optimal local properties are usually not orthotropic everywhere. This is shown in Fig. 20.

4.4
A 3D example. Optimal design of structural materials and topology

Finally we give a simple example to show the application of the energy-based model in 3D problem. Figure 20a shows a thick plate with simple supports on the corners of its lower surface and a concentrated load p applied on the centre H of its upper surface $DEFG$. According to the symmetry of the structure and load, in the

optimal design, only one quarter of the original design domain needs to be considered, with proper constraints introduced into the symmetric plane. This is shown in Fig. 20b. The initial materials uniformly distributed in design domain are isotropic materials with Young's modulus $E = 2.3 \times 10^{10}$, Poisson's ratio $\nu = 0.3$. The one quarter of original design domain is divided by $15 \times 15 \times 15$ mesh, see Fig. 21. Eight-node hexahedral isoparametric elements are employed to map each sub-cuboid divided. The total number of elements, nodes and DOF are, respectively, 3375, 4096 and 12288.

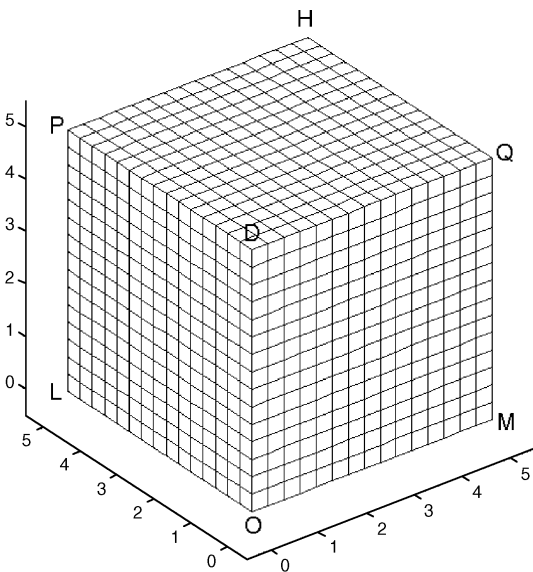


Fig. 21 3D mesh ($15 \times 15 \times 15$)

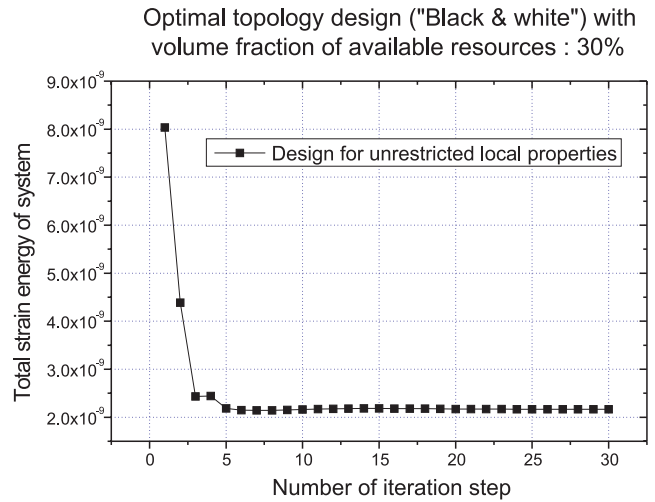


Fig. 22 Variation of total strain energy with iteration

Figure 22 shows the variation of the total strain energy with iteration in the optimal topology design for unrestricted local properties. The volume fraction of available resources is 30%. Figure 23 shows the associated optimal topology with optimal materials from different views. The numbers of independent material components are 21 for 3D cases. Similarly, the optimal materials can be identified as orthotropic materials in point-wisely varied principal coordinates.

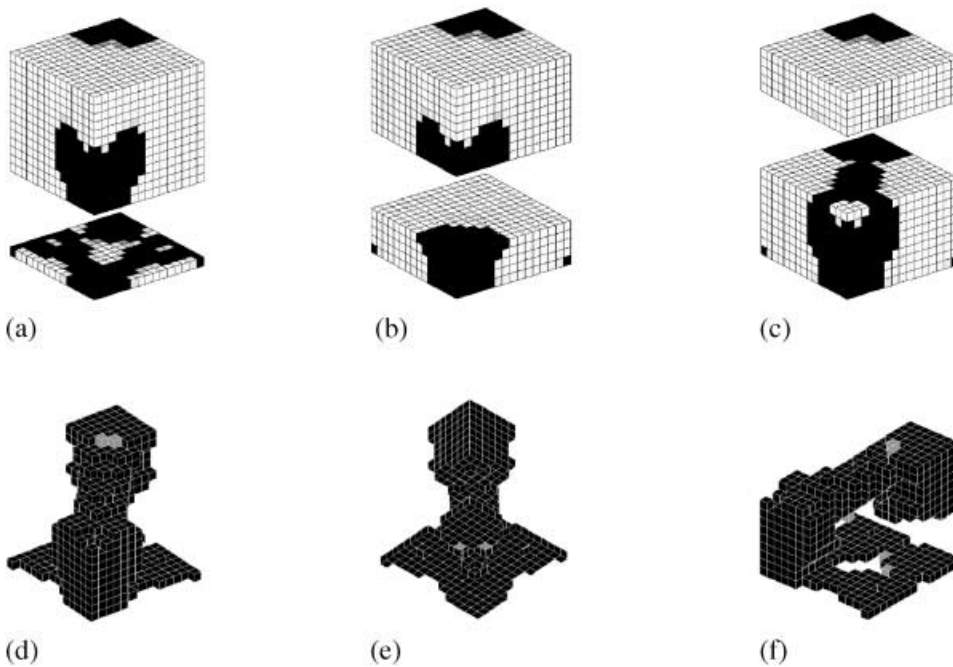


Fig. 23 Optimal topology with optimal local properties (“black & white”, volume fraction 30%; only one quarter of original structure from symmetry shown)

5 Summary

The material covered in this paper makes use of an approach to design that incorporates the capability to perform optimization at the level of the modulus tensor. Results obtained from an implementation of the model for computational solution are presented for problems in 2D and 3D, showing designs in ‘shades of gray’ and for zero-one topology design. Designs are demonstrated in the setting where material properties are taken to be fixed isotropic, designable isotropic, or “unrestricted”. Designs predicted for the latter case indicate that significant gains are possible with improvement in materials.

Several features identified with the formulation for and treatment of design at this elemental level may be of interest.

- Since results obtained where the modulus tensor is unrestricted predict the absolute best design from among the set of all admissible structures covered by the assumed broad theory of mechanics (here the classical linear elasticity model) and within a uniformly prescribed limit on the assumed cost, they provide a benchmark value or bound on the particular design objective, i.e. the measure of structural performance. As an example, the continuum design associated with the optimal unrestricted material tensor field for the chosen objective – determined for a specified cost and within prescribed spatial boundaries – bounds the efficiency of all finite trussed structures within the set defined by the same physical space, objective, and bound on total cost.

- Because the model accommodates infinitely variable material properties, it is elemental as well in the respect that both the applicable mechanics and the design optimization for all possible material composites are implicit within it. This may be appreciated through separate consideration of the mechanics and the design aspects of the formulation. For the former, it is necessary only to confirm (in the usual ways) that considerations of equilibrium, kinematic consistency, and constitutive properties for classical elastostatics are properly represented in the formulation. For the design part of the problem formulation, it may be verified as well that a characterization for optimal design of one or another among forms of composite structure may be obtained by an interpretation of the modulus tensor to represent a mixture, combined with imposition of a suitable set of constraints on the original unrestricted tensor formulation. As an example, designation of the appropriate constraint on local properties leads to the best design composed of isotropic material. As another example, a technique is available to predict the optimal design of composites composed of some combination of two or more functionally-graded materials. The counterpart problem in finite form, namely the optimal distributions of separate materials forming the best composite for a finite truss also may be treated using the same type of formulation.
- The computational effort required for the numerical solution of design problems to predict the optimal structure having infinitely variable material properties is of the same order as that required for the solution of the respective, more familiar material distribution design problem. The same comment applies

to the optimal topology design problem. Specifically, the computational effort in the more general problem equals “ n ” times the effort for the comparable material distribution prediction, where “ n ” equals the number of scalar variables required to define the more general material. In the unrestricted tensor case, “ n ” equals six or twenty-one in 2D and 3D, respectively.

- Since topology designs may be predicted in all cases from the continuum results, the present approach provides a viable alternative to familiar approaches (Rozvany 2001a,b) for topology design.

Acknowledgements The effort leading to the results reported here was supported by the Ford Motor Company – Scientific Research Laboratories, Dearborn, Michigan.

References

- Bendsøe, M.P.; Guedes, J.M.; Haber, R.B.; Pedersen, P.; Taylor, J.E. 1994: An analytical model to predict optimal material properties in the context of optimal structural design. *J. Appl. Mech.* **61**, 930–937
- Cherkaev A. 2000: *Variational methods for structural optimization*. Berlin, Heidelberg, New York: Springer
- Foldager, J.P. 1999: *Design of composite structures*. Ph.D Dissertation, Special Report No. 39, Institute of Mechanical Engineering, Aalborg University, Denmark
- Guedes, J.M.; Taylor, J.E. 1997: On the prediction of material properties and topology for optimal continuum structures. *Struct. Optim.* **14**, 193–199
- Liu, B.; Haftka, R.T.; Akgun, M.A. 2000: Two-level composite wing structural optimization using response surfaces. *Struct. Optim.* **20**, 87–96
- Michell, A.G.M. 1904: The limits of economy of material in framed structures. *Phil. Mag.* **6**, 589–597
- Olhoff, N.; Jacobsen, J.B.; Ronholt, E. 1997: Three-dimensional structural topology and layout optimization based on optimum microstructures. *Extended Abstracts of WCSMO-2* (held in Zakopane, Poland, May 26–30)
- Pedersen, P. 1993: Optimal orientation of anisotropic materials/optimal distribution of anisotropic materials, optimal shape design with anisotropic materials. In: Rozvany, G.I.N. (ed.) *Optimization of large structural systems* (Proc. NATO/DFG ASI, held in Berchtesgaden, Germany 1991). Dordrecht: Kluwer
- Prager, W. (ed.) 1974: *Introduction to structural optimization*. Course No. 212, International Center for Mechanical Sciences, Udine. Berlin, Heidelberg, New York: Springer
- Prager, W.; Rozvany, G.I.N. 1977: Optimization of structural geometry. In: Bednarek, A.R.; Cesari, L. (eds.) *Dynamical systems*, pp. 265–293. New York: Academic Press
- Rodrigues, H.; Soto, C.A.; Taylor, J.E. 1999: A design model to predict optimal two-material composite structures. *Struct. Optim.* **17**, 186–198
- Rozvany, G.I.N. 1976: *Optimal design of flexural systems*. Oxford: Pergamon
- Rozvany, G.I.N. 2001a: Aims, scope, methods, history and unified terminology of computer-aided topology optimization in structural mechanics. *Struct. Optim.* **21**, 90–108
- Rozvany, G.I.N. 2001b: Stress ratio and compliance based methods in topology optimization – a critical review. *Struct. Optim.* **21**, 109–119
- Sigmund, O. 2000: A 99 line topology optimization code written in Matlab. *Struct. Optim.* **21**, 120–127
- Taylor, J.E. 1998: An energy model for the optimal design of linear continuum structures. *Struct. Optim.* **16**, 116–127
- Taylor, J.E. 2000: Addendum to: an energy model for the optimal design of linear continuum structures. *Struct. Optim.* **19**, 317–320
- Taylor, J.E.; Washabaugh, P.D. 1995: A generalized expression of cost for prediction of the optimal material properties tensor. In: Monteiro Marques, M.D.P.; Rodrigues, J.F. (eds.) *Trends in application of mathematics to mechanics*. Essex: Longman